Understanding the stable boron clusters: A bond model and first-principles calculations based on high-throughput screening

Shao-Gang Xu,[1] Yu-Jun Zhao,[1,2] Ji-Hai Liao,[1] and Xiao-Bao Yang[1,2,a)]
[1]*Department of Physics, South China University of Technology, Guangzhou 510640, People's Republic of China*
[2]*Key Laboratory of Advanced Energy Storage Materials of Guangdong Province, South China University of Technology, Guangzhou 510640, People's Republic of China*

(Received 9 April 2015; accepted 22 May 2015; published online 4 June 2015)

The unique electronic property induced diversified structure of boron (B) cluster has attracted much interest from experimentalists and theorists. $B_{30–40}$ were reported to be planar fragments of triangular lattice with proper concentrations of vacancies recently. Here, we have performed high-throughput screening for possible B clusters through the first-principles calculations, including various shapes and distributions of vacancies. As a result, we have determined the structures of B_n clusters with n = 30–51 and found a stable planar cluster of B_{49} with a double-hexagon vacancy. Considering the 8-electron rule and the electron delocalization, a concise model for the distribution of the 2c–2e and 3c–2e bonds has been proposed to explain the stability of B planar clusters, as well as the reported B cages. © *2015 AIP Publishing LLC.* [http://dx.doi.org/10.1063/1.4922059]

I. INTRODUCTION

The variety of carbon nanotubes,[1] hollow cages,[2] and planar clusters[3,4] is attributed to the stable sp^2 hybridizations of carbon. All these nanostructures have similar motifs with the planar sheet of graphene.[5–7] Boron is the neighbor of carbon in the periodic table; however, neither hexagonal nor triangular boron nanotubes[8–10] or clusters[11–15] were found to be stable. Recent computational prediction of B_{80}[16] suggests that a triangular boron lattice with proper vacancies should be more stable, leading to extensive searches of possible planar sheets[17–19] and nanotubes[9,20–22] with various concentration and distribution of vacancies.[17,23]

Experimental observations have shown a striking evolution of B clusters with the increasing size. Twelve B atoms form a highly symmetric icosahedral cluster in the bulk structure,[24,25] while the most stable B_{12}[26] is a planar triangular fragment for isolated clusters. Similarly, the B_{16}^- and B_{16}[27] are also fragments from the triangular lattice, while B_{17}^-, B_{18},[28] B_{19},[29] B_{21},[30] B_{23},[31] and B_{24}[32] possess planar or quasi-planar structures with tetragonal or pentagonal defects. Besides the chiral cluster of B_{30},[33] the B_{36}[34] is found to be a highly stable cluster with perfect C_{6V} hexagonal symmetry, while the low-lying isomers of B_{35}[35] and B_{40}[36] are planar triangular fragments with double hexagonal vacancies. Besides aromatic and antiaromatic electronic properties analogous to hydrocarbons, the planar or quasi-planar boron clusters offer a rich variety of aromaticity (such as double aromatic and double antiaromatic), which has been established by using the photoelectron spectroscopy and *ab initio* calculations.[37] The stability of boron cluster can be explained by a novel chemical bond model, leading to the design of new boride materials with high coordinated borometallic molecules.[38]

It is still a challenge to determine the structures of B clusters due to the electron deficiency, since the variety of candidates grows as the number of B atoms increases. Though the planar clusters would be transformed into hollow cages (such as B_{38}[39] and B_{40}[36]), the investigation of planar structures would be crucial to the possible one-atom-thick B sheet,[17,18,23] which has been intensively studied in the past decades. Meanwhile, the bonding among B atoms is also complicated, though it can be analyzed through the adaptive natural density partitioning (AdNDP) method,[40] localizing the computed density matrix into n-center two-electron (nc–2e) bonds with n ranging from one to the total number of atoms in the molecule. For delocalized bonding among B atoms, the computational cost would be sharply increased with large n, bringing obstacles for the understanding of B clusters' stabilities. According to the B clusters found experimentally,[26,33,34,36] the stable planar structures should be fragments of triangular lattices, and the proper hexagonal vacancies would be necessary to enhance the structural stabilities as the number of B atoms increases. However, there are several issues to be concerned: (i) What are the shapes of fragments and the optimal number of vacancies for a given number of B atoms? (ii) With given shapes and the number of vacancies, which distribution of vacancies corresponds to the ground states? (iii) For the stable B clusters, is there any simple picture to describe the bonding among B atoms?

In this paper, we have performed high-throughput screening[41] for the possible B clusters from the fragments of triangular lattice, including various shapes and distributions of vacancies. We have found a new stable planar cluster of B_{49} with a double-hexagon vacancy, demonstrating that both the distribution and concentration of vacancies are crucial to the stability of B planar clusters. Notably, we have proposed a simple model for describing the two-center two-electron (2c–2e) and three-center two-electron (3c–2e) bonds' distribution to demonstrate why these B planar clusters are stable. The high

a)E-mail address: scxbyang@scut.edu.cn

stability of recently observed B_{40}[36] cage is also explained by our model.

II. COMPUTATIONAL METHODS

We focused on the planar B_n cluster consisted of the triangular lattice shown in Fig. 1. Combined with a congruence check, we obtained all the possible isomers for the fragments of triangular lattice for given number of atoms. For example, there are seven isomers of triangular fragments with four atoms (marked as m_{1-7}). The number of isomers increases as exponential function with n and reaches 30 490 when n = 10, as shown in Fig. S1.[42] For practical clusters, the candidates with least bonds should not be stable such as m_3–m_7, though the number of these ones is rather large (shown in Fig. S1[42]). We might limit candidates if we only consider the ones with most bonds; however, we would miss most of them which would be possibly stable. Meanwhile, candidates similar to m_2 with moderate bonds would not be stable either, since there are atoms with only one nearest neighbor. Besides, we can reduce the number of candidates a little if considering the candidates with enclosed profiles (each atom with more than one nearest neighbor). To enhance the efficiency of screening, more constraints should be applied to reduce the number of candidates and to avoid missing the possibly stable ones.

Based on the B_{30-40} synthesized by the experiment, the profile shapes of stable structure are convex with proper distribution of vacancies, where every atom owns three nearest neighbors at least. We set n_1 as the maximum number of atoms along the horizontal direction, and the profiles of isomers can be identified with the description of $\{n_1n_2n_3\}$ (n_2 and n_3 represent the number of atoms in the bottom and top row, respectively, $n_1 > n_2 \geq n_3$). The minimum of n_1 should be 3, and there is only one candidate of {322}. When n_1 = 4, there are three different profiles ({432}, {433}, and {422}) as shown in Fig. 1. For a given profile, we considered the candidates with various number and distribution of vacancies (one candidate for the {855} with three vacancies was shown as an example). We focused on the B_n clusters with n = 30–51 and obtained the candidates as follows: (i) start with n_1 = 6–9 and consider all possible n_2/n_3 to pre-screen the profiles; (ii) with given profiles, we introduce the vacancy one by one and consider all possible isomers by ergodicity; (iii) we stop introducing more vacancies when the average total energies increase with the increment of vacancies. We have applied a high-throughput screening for stable B cluster among the candidates of the fragments of triangular lattice. With one or two vacancies, the number of isomers is around 200 and we managed to calculate all their total energies. However, the number of isomers for B_{51} is 2269 when the candidates contain three vacancies, and we adopted an energy model to describe the structural stabilities, calculating the structures with higher ranking by first-principle methods.

The first-principles calculations of B planar candidates were based on the density functional theory (DFT) implemented in the Vienna *ab initio* simulation package (VASP)[43,44] method. The projector augmented wave (PAW) and the Perdew–Burke–Ernzerhof (PBE) of Generalized Gradient Approximation (GGA) functional[45,46] were employed for the total energies calculations. The energy cutoff was 480 eV, and the criteria of the forces were set to be 0.02 eV/Å for all atoms. Various values of energy cutoff from 450 eV to 550 eV were tested and the energy difference per atom was found to be within 0.15 meV. To avoid the cell-to-cell interactions, the vacuum distance was carefully tested. We also used the DMol[3] (Refs. 47 and 48) code combined with exchange-correlation function of GGA(PBE) for comparison. In addition, we have performed the calculation with the functional of Heyd-Scuseria-Ernzerhof (HSE06),[49,50] to obtain the energy gaps between the highest occupied molecular orbital (HOMO) and lowest unoccupied molecular orbital (LUMO). The HSE06 calculated gap of α-rhombohedra boron[51] was found to be 2.6 eV, in good agreement with the electron energy loss experiment observations (2.4 eV).[52]

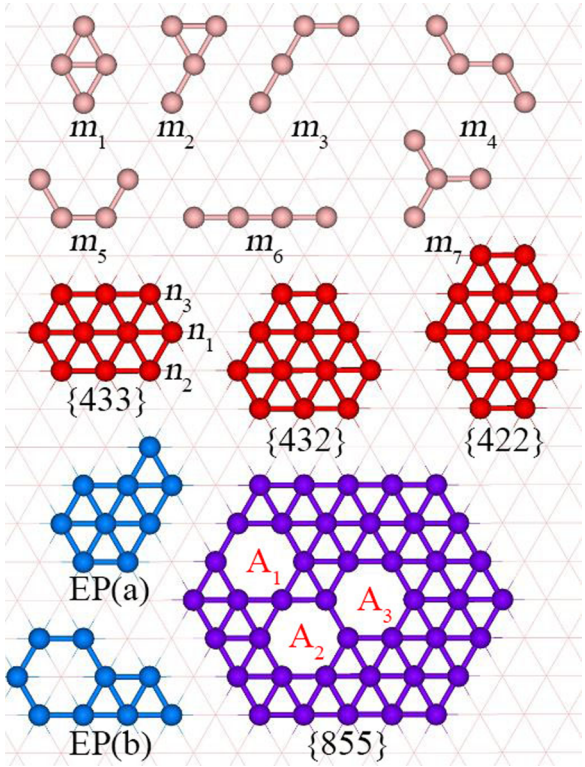

FIG. 1. Possible candidates for B_n clusters consisted of the triangular lattice. All isomers for n = 4 are marked as m_1–m_7. Two examples of B_9 clusters with enclosed profiles (EP) are shown. B_n clusters with convex profiles are indicated with $\{n_1n_2n_3\}$, there are {422}, {432}, and {433} for n_1 = 4. In the profile of {855}, A_1, A_2, and A_3 stand for the possible positions for vacancies.

III. RESULTS AND DISCUSSIONS

As shown in Fig. 2, we have calculated the average formation energies (E_f) of 3596 candidates for B_n clusters (n = 30–51), including various triangular fragments with/without vacancies. The stable structures for B_{30-51} clusters with the formation energies are shown in Fig. S2.[42] For the fragments without vacancies, E_f decreases first as the size increases and gradually increases when n > 46. Thus, we have considered the fragments with one vacancy and found that the stable B_{30} and B_{36} are planar clusters in agreement with the experimental observations.[33,34] Besides, both B_{41} and B_{46} are triangular fragments with one vacancy, while the average formation

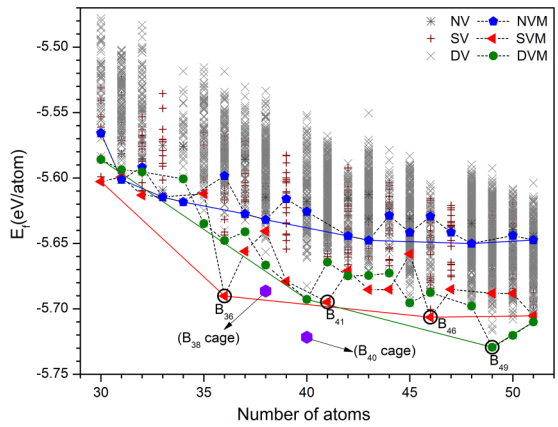

FIG. 2. The formation energy (E_f) of planar B_n clusters as a function of size. The cage of B_{38} and B_{40} is shown for comparison. The isomers with none vacancies (NV), single vacancy (SV), and double vacancies (DV) are indicated with ∗, +, and ×, respectively. Full pentagons, triangles, and circles guided with three dashed lines are for the lowest candidates with the same number of B atoms for NV, SV, and DV, respectively, which are marked as (NVM, SVM, and DVM), and the blue, red, and green solid lines are the convex profile of curves.

energy of B_{46} corresponds to the local minimum for such type of candidates. We have considered the structures with two vacancies and obtained stable B_{40}[36] and B_{35}[35] as confirmed in experiments. Interestingly, we have found a highly stable magic cluster of B_{49}, which contains a double-hexagonal vacancy in the center. We have also calculated the average formation energies of stable cage (B_{38} and B_{40}) for comparison, which have been predicted by theoretical studies[39] and experimental observations.[36] The planar clusters might be transformed into hollow cages as the size increases; however, the stable B_{49} with two vacancies indicates that there might be stable planar B clusters with proper profile and distributions of vacancies.

Both experimental and theoretical studies showed that the vacancies would appear in triangular fragments to enhance the stabilities as the number of B atoms increased. However, we cannot prejudge how many vacancies are required for given profiles of triangular fragments. For example, we found a B_{37} cluster of {744} with the C_{6v} symmetry which contains no vacancy, and its E_f is −5.586 eV/atom. When there is one vacancy, the average formation energies were from −5.577 eV/atom to −5.690 eV/atom, depending on the positions of the vacancy. The most stable one corresponds to the vacancy at the center and the cluster maintains the C_{6v} symmetry. In general, the B clusters should be not stable if there are six nearest neighbors for every B atom. Thus, we propose an electrostatic energy model to describe the structural stabilities: the B atoms with five nearest neighbors are electrically neutral, while the B atoms are positively (negatively) charged when the number of nearest neighbors is less (more) than five. The electrostatic energy is expressed as $\sum_{i=1}^{n-1}\sum_{j>i}^{n} q_i * q_j/R_{ij}$, where R_{ij} is the distance between the ith atom and jth atom. The q_i of each B atom is rescaled to maintain the charge neutrality of the whole cluster. Note that there is a positive correlation between the average formation energies and the model energies as shown in Fig. 3. Meanwhile, all B_{35} isomers with two vacancies in the profile of B_{37} are less stable than B_{36}. Thus, we can conclude that B_{36} is the magic cluster as verified in the recent experiment.

Similarly, we confirmed that B_{41} and B_{46} are magic clusters with one vacancy, since the clusters in the same profile with more vacancies would become unstable (shown in Fig. S2[42]). B_{36} was regarded as the biggest stable planar cluster with only one hexagonal vacancy. However, we have found that B_{46} is highly stable and symmetrical with one hexagonal vacancy. At the same time, our result indicates that B_{46} is the optimal structure with only one hexagonal vacancy. For the triangular fragment of {966} with 51 B atoms, we found that B_{49} with a double-hexagonal vacancy is highly stable. For comparison, we also consider B_{48} with three vacancies, though the number of three vacancies isomers is far more than that of the ones with double-vacancy. For B clusters with one or two vacancies, there is an approximate linear relationship between the average energy and the electrostatic potential from model analysis. As the B_{48} cluster with three vacancies has 955 isomers, we scan all the isomers by the electrostatic potential model and calculated the total energies of the 100 lowest electrostatic potential structures by DFT. As the number of vacancies increases, the correlation between the average total energies and the model energies is not as good as that for the clusters with one or two vacancies, which might be due to the many-body interactions among B atoms.

Table I in the supplementary material[42] shows the HOMO-LUMO (H-L) energy gaps of B_n clusters from various methods, which indicate the same tendency for these stable B_n clusters. In general, the large H-L gaps indicate the high stability of clusters. The gap of planar B_{36} is around 1.7 eV according to HSE calculations and the one of B_{40} cage is around 2.4 eV. We have found that the gap of B_{46} is 0.80 eV, while the ones of B_{41}^+ and B_{49}^+ are around 1.5 eV and 1.2 eV,

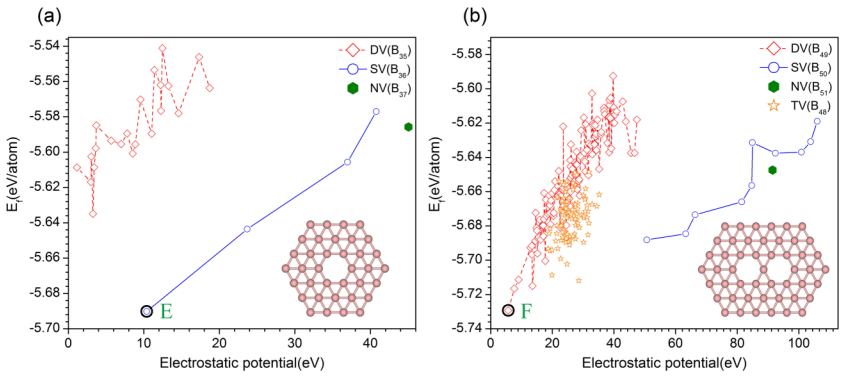

FIG. 3. The relationship between electrostatic potential and formation energies (E_f) for B_n planar clusters with given profiles: (a) {744}; (b) {966}. The isomers with NV are marked with solid hexagons, while the ones with SV, DV, and triple vacancies (TV) are indicated with empty circles, rhombuses, and penta-stars, respectively.

respectively. Thus, the planar B_{41}^+, B_{46}, and B_{49}^+ clusters should be highly stable.

To understand the stabilities of magic B planar clusters, we have investigated the bonding among B atoms and proposed a distribution model based on 2c–2e bonds and 3c–2e bonds. There are two main assumptions in our model: (i) s 2c–2e bonds and t 3c–2e bonds are introduced for B_n clusters to satisfy the 8-electron rule for every B atom (i.e., $2s + 2t = 3n$ and $4s + 6t = 8n$), indicating that $s = 0.5n$ and $t = n$, respectively [($s = 0.5(n - 3)$ and $t = n + 1$ for B_n^+ clusters]; (ii) the distribution of 2c–2e and 3c–2e bonds should be in agreement with the charge difference, as well as the configuration's symmetry. According to our model, we can determine the bond distributions and ensure every B atom satisfies the 8-electron rule. The element B in the periodic table is located in the boundary of metals and nonmetals, indicating its bonding should be characterized with both localization and delocalization. The 8-electron rule indicates the localization, while the delocalization has been also verified by the π bonding in planar B clusters. Thus, we minimize the variance of 2c–2e and 3c–2e bonds' distribution for describing the delocalized bonding. Suppose that there are s_0 ($s_0 \geq s$) sites for the 2c–2e bonds at the edge and t_0 ($t_0 \geq t$) sites for the 3c–2e bonds at the triangles inside. The variance of distribution is expressed as $\delta = \sum_{i=1}^{s_0} \left(s_i - \frac{s}{s_0}\right)^2 + \sum_{j=1}^{t_0} \left(t_j - \frac{t}{t_0}\right)^2$, where s_i and t_j are the occupation of 2c–2e and 3c–2e bonds at the edge and triangles, respectively.

Figure 4(a) shows the charge difference of B_{36}, which shows a six-fold symmetry as well as its geometry. The 3c–2e bonds are necessary to maintain the 8-electron rule for every B atom; however, the distribution of 2c–2e and 3c–2e bonds cannot be simply determined in B clusters. Taking the neutral B_{36} as an example, there are 24 edge bonds for 18 2c–2e bonds and 48 triangles for 36 3c–2e bonds. Considering s_i and t_j of either 0 or 1, we have enumerated all the possible distributions and found that two solutions maintain the six-fold symmetry as shown in Figs. S4(a) and S4(b).[42] Both the variances for these two distributions are 13.5, which are quite distinct compared to the charge difference (shown in Fig. 4(a)). Interestingly, we have found another distribution from the average of these two distributions with $\delta = 4.5$ as shown in Fig. 4(b). In such a case, the occupation of edge bonds and triangles could be 0, 1/2, and 1, which is in better agreement with the charge difference. The 1/2 occupation of 3c–2e and 2c–2d bond would provide 1 electron for each B atom, respectively. In the central vacancy, there are only three 2c–2e bonds in one hexagon and these bonds are delocalized to produce six 2c–2e bonds with the occupations of 1/2. Note that the number of 2c–2e and 3c–2e bonds still satisfies the above equations and every B atom obeys the 8-electron rule.

Figures 4(c) and 4(d) show the charge difference of B_{49}^+ and the model analysis of 2c–2e and 3c–2e bonds' distribution, where there are mirror symmetries along both the horizontal and perpendicular directions. Note that there is no solution for B_{49}^+ with the occupation of 0 and 1 which meets the symmetry. We, however, found several pairs of degenerate solutions ($\delta = 19.562$) with mirror symmetry only along the perpendicular directions (shown in Fig. S4[42]). The minimum δ of these distributions with the occupations of 0, 1/2, and 1 is 8.062, containing 38(12) bonds of 3c–2e(2c–2e) with the occupations of 1, and 24(22) bonds of 3c–2e(2c–2e) with the occupations of 1/2. We have applied the similar operations for B_{41}^+ and B_{46}, obtaining the solutions with the occupations of 0, 1/2, and 1 from the average of the solutions with the occupations of 0 and 1 (shown in Fig. S5[42]). Though the distribution variances decrease, there are rather obvious deviations compared to the charge difference. We have found that the solutions based on the occupation of 1/2 are in better agreement with the charge difference, containing smaller variances of distribution (as shown in Fig. S6[42]).

Generally, we might consider a continuous model for the occupations to minimize the variances of distribution.

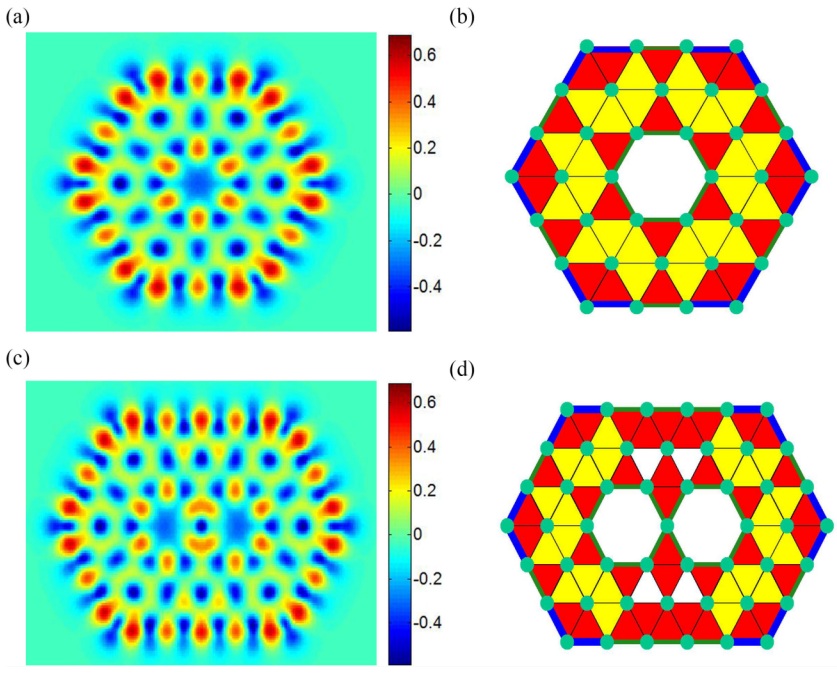

FIG. 4. Bonding analysis for the stable B_{36} and B_{49}^+: ((a)-(c)) charge difference; ((b)-(d)) possible distributions of 2c–2e and 3c–2e bonds. The thick blue/thin green lines are indicated for 2c–2e bonds with the occupations of 1 and 1/2, and the red/yellow triangles are for 3c–2e bonds with the occupations of 1 and 1/2.

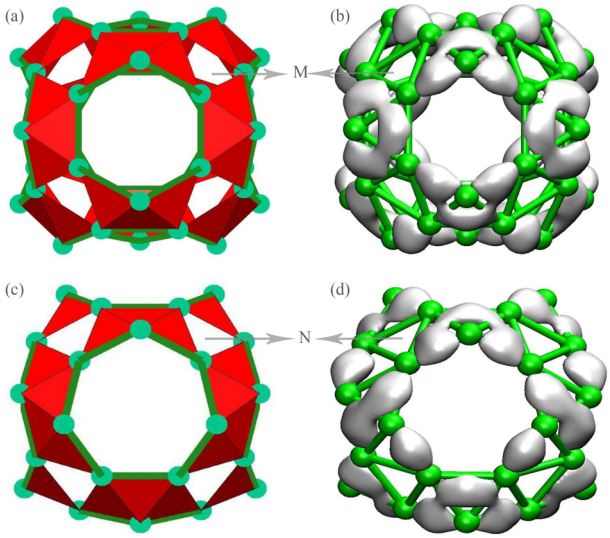

FIG. 5. Bonding analysis for the stable B_{40}: ((a) and (c)) the distributions of 2c–2e and 3c–2e bonds; ((b) and (d)) isosurface of charge difference of B_{40} cage. (a) and (b) are the top view; (c) and (d) are the side view. The thin green lines are indicated for 2c–2e bonds with the occupations of 1/2, and the red triangles are for 3c–2e bonds with the occupations of 1.

However, it would lead to another complicate problem of optimization and miss a clear picture to describe the bonding among B atoms. For simplicity, we consider the occupations of 0, 1/2, and 1, and extend our model to analyze the highly stable B_{40} cage observed in the recent experiment.[36] As shown in Figs. 5(a) and 5(c), our model analysis show that there are 40 2c–2e bonds with the occupations of 1/2, located at the edges of two hexagons and four heptagons. Similar to the planar B_{36}, there are six/seven electrons in the hexagons/heptagons are delocalized to produce six/seven 2c–2e bonds with the occupations of 1/2, respectively. There are 40 3c–2e bonds with the occupations of 1, and eight empty triangles with no bonds' distributions, which ensure the 8-electrons rule for every B atom. According to the charge difference (shown in Figs. 5(b) and 5(d)), we found that there was no charge distribution in eight triangles (marked by M and N), whose three vertexes are from one hexagon and two separate heptagons. Our model analysis, in good agreement with the charge difference, proposes an explanation for the high stability of B_{40} cage. Our model for describing the 2c–2e and 3c–2e bonds' distribution is found to be universal for the high stabilities of B_n clusters, including planar ones and cages.

IV. CONCLUSION

In summary, we have investigated the structural stabilities of B_n (n = 30–51) clusters, based on high-throughput screening combined with the first-principles calculations. Besides verifying that B_{30} and B_{36} are stable clusters among the possible candidates from triangular lattice fragments, we found a highly stable magic cluster of B_{49} with a double-hexagonal vacancy in the center. Notably, we have proposed an effective model for describing the 2c–2e and 3c–2e bonds' distribution, which is in agreement with the charge difference satisfying the geometry's symmetry. In stable B clusters, every B atom meets the 8-electron rule and the variance of bonds' distribution should be minimized. This is found to be universal for the high stabilities of planar clusters (B_{36} and B_{49}^+) and cages (B_{40}).

ACKNOWLEDGMENTS

This work was supported by NSFC (Grant Nos. 11474100 and 11174082) and Guangdong Natural Science Funds for Distinguished Young Scholars (Grant No. 2014A030306024). The computer times at National Supercomputing Center in Shenzhen (NSCCSZ) and ScGrid of the Super-computing Center, Computer Network Information Center of CAS are gratefully acknowledged.

[1]S. Iijima, Nature **354**, 56 (1991).
[2]H. W. Kroto, J. R. Heath, S. C. O'Brien, R. F. Curl, and R. E. Smalley, Nature **318**, 162 (1985).
[3]R. Saito, M. Yagi, T. Kimura, G. Dresselhaus, and M. Dresselhaus, Mol. Cryst. Liq. Cryst. Sci. Technol., Sect. A **340**, 71 (2000).
[4]S. K. Singh, M. Neek-Amal, and F. Peeters, Phys. Rev. B **87**, 134103 (2013).
[5]K. S. Novoselov, A. K. Geim, S. V. Morozov, D. Jiang, M. I. Katsnelson, I. V. Grigorieva, S. V. Dubonos, and A. A. Firsov, Nature **438**, 197 (2005).
[6]K. S. Novoselov, A. K. Geim, S. Morozov, D. Jiang, Y. Zhang, S. Dubonos, I. Grigorieva, and A. Firsov, Science **306**, 666 (2004).
[7]K. Novoselov, D. Jiang, F. Schedin, T. Booth, V. Khotkevich, S. Morozov, and A. Geim, Proc. Natl. Acad. Sci. U. S. A. **102**, 10451 (2005).
[8]M. Evans, J. Joannopoulos, and S. Pantelides, Phys. Rev. B **72**, 045434 (2005).
[9]D. Ciuparu, R. F. Klie, Y. Zhu, and L. Pfefferle, J. Phys. Chem. B **108**, 3967 (2004).
[10]I. Boustani and A. Quandt, Europhys. Lett. **39**, 527 (1997).
[11]I. Boustani, A. Quandt, E. Hernández, and A. Rubio, J. Chem. Phys. **110**, 3176 (1999).
[12]I. Boustani, Phys. Rev. B **55**, 16426 (1997).
[13]I. Boustani, Surf. Sci. **370**, 355 (1997).
[14]I. Boustani, A. Rubio, and J. A. Alonso, Chem. Phys. Lett. **311**, 21 (1999).
[15]S. Chacko, D. Kanhere, and I. Boustani, Phys. Rev. B **68**, 035414 (2003).
[16]N. G. Szwacki, A. Sadrzadeh, and B. Yakobson, Phys. Rev. Lett. **98**, 166804 (2007).
[17]X. J. Wu, J. Dai, Y. Zhao, Z. W. Zhuo, J. L. Yang, and X. C. Zeng, ACS Nano **6**, 7443 (2012).
[18]E. S. Penev, S. Bhowmick, A. Sadrzadeh, and B. I. Yakobson, Nano Lett. **12**, 2441 (2012).
[19]T. R. Galeev, Q. Chen, J. C. Guo, H. Bai, C. Q. Miao, H. G. Lu, A. P. Sergeeva, S. D. Li, and A. I. Boldyrev, Phys. Chem. Chem. Phys. **13**, 11575 (2011).
[20]X. Yang, Y. Ding, and J. Ni, Phys. Rev. B **77**, 041402 (2008).
[21]B. Kiran, S. Bulusu, H.-J. Zhai, S. Yoo, X. C. Zeng, and L.-S. Wang, Proc. Natl. Acad. Sci. U. S. A. **102**, 961 (2005).
[22]P. Manuel, Molecules **15**, 8709 (2010).
[23]X. Yu, L. Li, X. Xu, and C. Tang, J. Phys. Chem. C **116**, 20075 (2012).
[24]A. Masago, K. Shirai, and H. Katayama-Yoshida, Phys. Rev. B **73**, 104102 (2006).
[25]M. Fujimori, T. Nakata, T. Nakayama, E. Nishibori, K. Kimura, M. Takata, and M. Sakata, Phys. Rev. Lett. **82**, 4452 (1999).
[26]H. J. Zhai, B. Kiran, J. Li, and L. S. Wang, Nat. Mater. **2**, 827 (2003).
[27]A. P. Sergeeva, D. Y. Zubarev, H.-J. Zhai, A. I. Boldyrev, and L.-S. Wang, J. Am. Chem. Soc. **130**, 7244 (2008).
[28]A. P. Sergeeva, B. B. Averkiev, H. J. Zhai, A. I. Boldyrev, and L. S. Wang, J. Chem. Phys. **134**, 224304 (2011).
[29]W. Huang, A. P. Sergeeva, H. J. Zhai, B. B. Averkiev, L. S. Wang, and A. I. Boldyrev, Nat. Chem. **2**, 202 (2010).
[30]Z. A. Piazza, W. L. Li, C. Romanescu, A. P. Sergeeva, L. S. Wang, and A. I. Boldyrev, J. Chem. Phys. **136**, 104310 (2012).
[31]A. P. Sergeeva, Z. A. Piazza, C. Romanescu, W. L. Li, A. I. Boldyrev, and L. S. Wang, J. Am. Chem. Soc. **134**, 18065 (2012).
[32]I. A. Popov, Z. A. Piazza, W. L. Li, L. S. Wang, and A. I. Boldyrev, J. Chem. Phys. **139**, 144307 (2013).
[33]W. L. Li, Y. F. Zhao, H. S. Hu, J. Li, and L. S. Wang, Angew. Chem., Int. Ed. **53**, 5540 (2014).
[34]Z. A. Piazza, H. S. Hu, W. L. Li, Y. F. Zhao, J. Li, and L. S. Wang, Nat. Commun. **5**, 3113 (2014).

[35]W. L. Li *et al.*, J. Am. Chem. Soc. **136**, 12257 (2014).
[36]H. J. Zhai *et al.*, Nat. Chem. **6**, 727 (2014).
[37]A. N. Alexandrova, A. I. Boldyrev, H.-J. Zhai, and L.-S. Wang, Coord. Chem. Rev. **250**, 2811 (2006).
[38]A. P. Sergeeva, I. A. Popov, Z. A. Piazza, W. L. Li, C. Romanescu, L. S. Wang, and A. I. Boldyrev, Acc. Chem. Res. **47**, 1349 (2014).
[39]J. Lv, Y. C. Wang, L. Zhu, and Y. M. Ma, Nanoscale **6**, 11692 (2014).
[40]D. Y. Zubarev and A. I. Boldyrev, Phys. Chem. Chem. Phys. **10**, 5207 (2008).
[41]S. Curtarolo, G. L. Hart, M. B. Nardelli, N. Mingo, S. Sanvito, and O. Levy, Nat. Mater. **12**, 191 (2013).
[42]See supplementary material at http://dx.doi.org/10.1063/1.4922059 for Figure S1. We show the number of various triangular lattice fragments as a function of size. In Figure S2, we show the stable configurations of B_n clusters, and the relationship between electrostatic potential and formation energies (E_f) is shown in Figure S3. Table I shows HOMO-LUMO gaps for stable B_n clusters through various methods. Figures S4 and S5 show possible distributions of 2c–2e and 3c–2e bonds for the stable (B_{36}, B_{49}^+) and (B_{41}^+, B_{46}), respectively. In Figure S6, we show the charge differences and possible distributions of 2c–2e and 3c–2e bonds for the stable B_{41}^+ and B_{46}, based on the occupations of 0, 1/2, and 1.
[43]G. Kresse and J. Furthmüller, Phys. Rev. B **54**, 11169 (1996).
[44]G. Kresse and D. Joubert, Phys. Rev. B **59**, 1758 (1999).
[45]J. P. Perdew, K. Burke, and M. Ernzerhof, Phys. Rev. Lett. **77**, 3865 (1996).
[46]J. P. Perdew, K. Burke, and M. Ernzerhof, Phys. Rev. Lett. **80**, 891 (1998).
[47]B. Delley, J. Chem. Phys. **92**, 508 (1990).
[48]B. Delley, J. Chem. Phys. **113**, 7756 (2000).
[49]J. Heyd, G. E. Scuseria, and M. Ernzerhof, J. Chem. Phys. **118**, 8207 (2003).
[50]J. Paier, M. Marsman, K. Hummer, G. Kresse, I. C. Gerber, and J. G. Ángyán, J. Chem. Phys. **124**, 154709 (2006).
[51]D. W. Bullett, J. Phys. C: Solid State Phys. **15**, 415 (1982).
[52]M. Terauchi, Y. Kawamata, M. Tanaka, M. Takeda, and K. Kimura, J. Solid State Chem. **133**, 156 (1997).